Alexander David Hofer, BSc

Osmotic Pressure Cell for Intermolecular Forces

MASTER'S THESIS

to achieve the university degree of

Diplom-Ingenieur

Master's degree programme: Technical Physics

submitted to

Graz University of Technology

Supervisor

Assoc.Prof. Univ.-Doz. Dipl.-Ing. Dr.techn. Georg Pabst

Institute of Materials Physics

Graz, August 2018

AFFIDAVIT

I declare that I have authored this thesis independently, that I have not used other than the declared sources/resources, and that I have explicitly indicated all material which has been quoted either literally or by content from the sources used. The text document uploaded to TUGRAZonline is identical to the present master‘s thesis.

Date	Signature

Acknowledgment

This master thesis was accomplished with the kind support and help of many individuals. I would like to express my sincere thanks to all of them.

Foremost, I want to thank my supervisor Georg Pabst who literally always had an open office door whenever I needed guidance or had a question about my research. I would also like to thank him for giving me plenty of freedom for working independently on my thesis and encouraging me to study the field of Biophysics. As my professor and mentor, he taught me many things about both, scientific research and life in general, which made him a true teacher to me. Furthermore, I am so thankful to my colleges from the institute for their great support and their caring friendship. Several fruitful discussions and their academic advice helped me a lot to complete this thesis.

I am highly indebted to Anton Paar GmbH for providing their resources to construct and manufacture the osmotic pressure cell and its components. I would especially like to thank Petra Kotnik, Josef Gautsch, Julia Nigitz and the whole Anton Paar SAXS team for doing such a great job.

I am extremely grateful to my parents and family for their love and unfailing support, not only during the time of my research, but throughout my whole life. Most importantly, I wish to say thanks to my loving and supportive wife, Seulki, for her help and cheerful words, especially during the last weeks. Also thank you for reviewing my thesis.

Finally, my thanks go to all the people who supported me to complete this thesis.

This work is cordially dedicated to my father, whom it was not allowed to see my thesis completed.

Abstract

Forces and interactions are intimately related to physical properties of matter at diverse length and time scales. Hence, determination of these interactions provides detailed knowledge regarding the physics pertaining to a given material of interest. Of particular interest are intermolecular forces in soft condensed matter, including aqueous solutions of all types of colloidal particles (e.g. macromolecules), as they determine aggregation behavior, stability or shelf-live. Probing these forces remains a challenge, however. A full-scale measurement needs to involve length scales from hard wall /steric interactions at close contacts to soft impacts in very dilute systems in order to unravel the physical chemistry pertaining to the space wars of volume occupation and collision. Our goal is to construct an osmotic pressure cell which allows to perform simultaneous small-angle x-ray scattering (SAXS) experiments in order to probe intercolloidal distances at a set pressure. The osmotic cell will have several advantages as compared to conventional techniques, which apply osmotic stress by using large neutral polymers. These include ease of sample handling, experimental setup-time and material costs. Further, as compared to previous designs our cell should be able to fully explore pressures between 0.01 – 100 bar.

After manufacturing and installation of the osmotic pressure cell at a SAXS camera (SAXSpace) extensive test were performed using multilamellar vesicles composed of the membrane lipid dioleoyl phosphatidylcholine, whose lamellar repeat distance can be tuned by osmotic pressure. Tests included different semipermeable membranes and equilibration times and led to a redesign of the osmotic pressure cell. The new cell successfully retained the sample within the x-ray beam and allowed sample equilibration over several days. Lamellar repeat distances obtained in the osmotic pressure range of 1 - 20 bar were in direct agreement with

reference data from measurements with osmotic stress technique (using polyethylene glycol) of large molecular weight as osmolyte. Furthermore, suggestions for improving the whole measuring system have been worked out.

Kurzfassung

Kräfte und Wechselwirkungen sind eng mit physikalischen Eigenschaften von Materie auf verschiedenen Längen- und Zeitskalen verbunden. Daher liefert die Bestimmung dieser Wechselwirkungen detailliertes Wissen über die Physik des jeweiligen Materials. Von besonderem Interesse sind intermolekulare Kräfte in weicher Materie (Soft Condensed Matter), einschließlich wässriger Lösungen mit Kolloiden (z. B. Makromoleküle), da sie das Aggregationsverhalten, die Stabilität oder die Haltbarkeit bestimmen. Die Untersuchung dieser Kräfte bleibt jedoch eine Herausforderung, da eine vollständige Messung Längenskalen von sterischen (hard wall) Wechselwirkungen bei kleinen Abständen bis hin zu weichen Stößen in sehr verdünnten Systemen umfassen muss, um die physikalische Chemie der Volumenbelegung inklusive ihrer Konflikten und Kollision zu entschlüsseln. Das Ziel ist eine osmotische Druckzelle zu entwickeln, die gleichzeitige Kleinwinkel-Röntgenstreuung (SAXS) ermöglicht, um die intermolekularen Abstände von Kolloiden bei einem eingestellten Druck zu untersuchen. Diese osmotische Zelle wird gegenüber herkömmlichen Techniken, wie z.B. osmotischen Stress durch die Verwendung von großen neutralen Polymeren, mehrere Vorteile haben. Dazu gehören die einfache Probenhandhabung, kurze Messzeiten und geringe Materialkosten. Darüber hinaus sollte die Zelle in der Lage sein, verglichen zu früheren Entwürfen, Drücke zwischen 0,01 - 100 bar vollständig zu untersuchen.

Nach Fertigung und Installation der osmotischen Druckzelle in einer SAXS-Kamera (SAXSpace) wurden umfangreiche Tests unter Verwendung von multilamellaren Vesikeln durchgeführt. Diese Vesikel bestanden aus dem Membranlipid Dioleoylphosphatidylcholin und haben eine durch osmotischen Druck einstellbare lamellare Wiederholungsdistanz. Die Tests umfassten verschiedene semipermeable Membranen und Äquilibrierungszeiten, welche die Grundlagen für eine Neugestaltung der osmotischen

Druckzelle lieferten. Die neue Zelle behielt den Probenspiegel erfolgreich oberhalb des Röntgenstrahls und erlaubte die Probenäquilibrierung über mehrere Tage. Die lamellaren Wiederholungsabstände, die in einem osmotischen Druckbereich von 1 bis 20 bar gemessen wurden, stimmten mit Referenzdaten von osmotischen Stressmessungen (unter Verwendung von Polyethylenglycol mit hohem Molekulargewicht) überein. Darüber hinaus wurden Vorschläge zur Verbesserung des gesamten Messsystems erarbeitet.

Contents

List of Figures

List of Acronyms / Abbreviations

CE	Cellulose Esther
DOPC	dioleoylphosphatidylcholine
MLVs	multilamellar vesicles
MWCO	molecular weight cut off
OPC	osmotic pressure cell
OS	osmotic stress
PEG	polyethylene glycol
PES	polyethersulfone
RC	Regenerated Cellulose
SAXS	small-angle x-ray scattering
SDD	sample detector distance

1 Introduction

1.1 Motivation for Constructing an Osmotic Pressure Cell

Forces and interactions are intimately related to physical properties of matter at diverse length and time scales. Hence, determination of these interactions provides detailed knowledge regarding the physics pertaining to a given material. Of particular interest are intermolecular forces in soft condensed matter, including aqueous solutions of all types of colloidal particles (e.g. macromolecules), as they determine aggregation behavior, stability or shelf-live. Probing these forces remains a challenge, however. A full-scale measurement needs to involve length scales from close contact steric interactions at high pressure to soft impacts in very dilute systems at low pressure in order to unravel the physical chemistry pertaining to the space wars of volume occupation and collision. Several techniques have been developed to measure intermolecular forces, including atomic force microscopy / spectroscopy (AFM) [1], the surface force apparatus (SFA) [2] or more recently acoustic force spectroscopy (AFS) [3]. None of these techniques, however, provide simultaneous structural insight at the sub-nanometer length scales. X-rays, in turn are capable of probing this regime. Four decades ago Parsegian and coworkers developed the so called osmotic stress (OS) technique for measuring interactions between lipid membranes [4] (Fig. 1.1). The strategy of these experiments is to control water activity (osmotic pressure) by using a solution of large neutral polymers, which neither interact with membranes, nor are able to penetrate into the interstitial water layers in multilamellar aggregates. The distance between membranes set by the osmotic pressure exerted by the polymer solution is readily measured by small-angle x-ray scattering

(SAXS). Over the years, several groups have made use of this technique to determine interaction between several macromolecules, including DNA [5], proteins [6] or complex lipid mixtures [7], to name but a few.

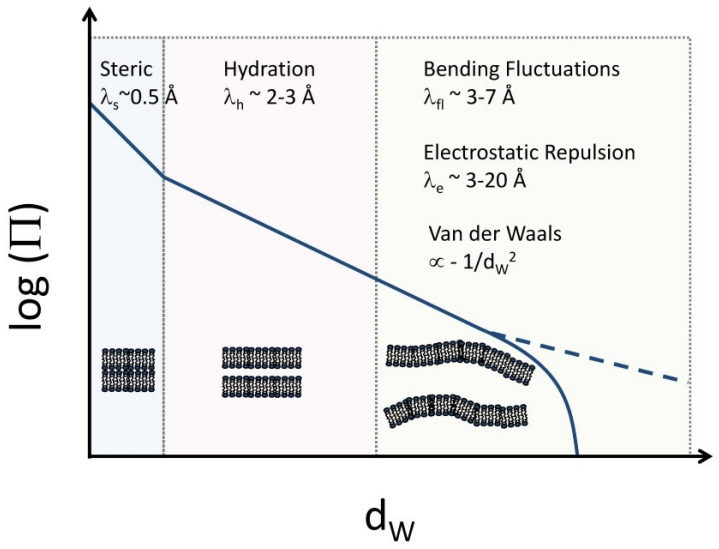

Figure 1.1: Generic interactions between lipid membranes as determined by OS measurements. Osmotic pressure Π sets the separation between bilayers d_W revealing three distinct regimes: (i) short-range: steric headgroup collisions, (ii) intermediate range: hydration interaction/swelling forces, (iii) long-range: balance of attractive van der Waals and repulsive fluctuation interactions or electrostatic forces.

Besides the broad applicability of the technique, there are however certain disadvantages. For example, a new sample needs to be prepared for each setting value of osmotic pressure, and samples need to be equilibrated for at least two days prior to SAXS experiments. To overcome this obstacle two groups have conceived osmotic pressure cells [8, 9], which allow to manually apply osmotic pressure. However, the designed either did not allow to achieve high pressures (50 – 100 bar) [8], or had problems in accurate measurements at low pressures (<3 bar) (Fig. 1.2) and equilibration times [9]. On the other hand, this range is important in order to probe the competition between long-range forces.

The new design of the osmotic pressure cell will avoid these problems

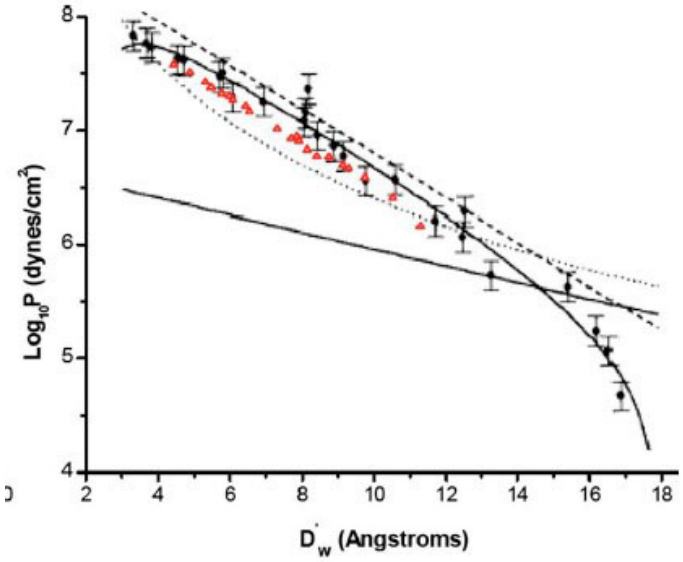

Figure 1.2: Osmotic pressure measurements on dioleoylphosphatidylcholine (DOPC) bilayers. Black dots show data obtained by the OS technique [10], red dots correspond to data from the osmotic pressure cell. Adapted from [9].

(i.e. probing from 0.01 bar – 100 bar), paving the way to new accurate measurements of intermolecular interactions not only for lipid membranes, but for colloids in general. It can be expected that this will be of significant interest to several groups in basic research, but also industry. The design will allow an installation of the cell not only within the SAXS product line of Anton Paar, but also at synchrotron beamlines. The later enables fast scans in osmotic pressures coupled to millisecond time-resolved scattering experiments in order to probe the kinetics of the interacting forces.

1.2 Measurement Setup

An essential component for performing an osmotic pressure measurement using SAXS - besides the osmotic pressure cell (OPC) itself - is a very accurate pressure supply system which is capable of providing a constant pressure over a wide range despite the demand for a high resolution.

Furthermore, an exact protocol for sample preparation and loading as well as proper filter membrane pretreatment is inevitable for obtaining reproducible experimental data.

1.2.1 Osmotic Pressure Cell (OPC)

The mechanical requirements for the OPC were initially defined by a sample volume of 10 - 50 µl. Keeping the amount of required material low - in this case multilamellar dioleoylphosphatidylcholine (DOPC) vesicles - saves material cost since high concentrated samples have to be used in the OPC.

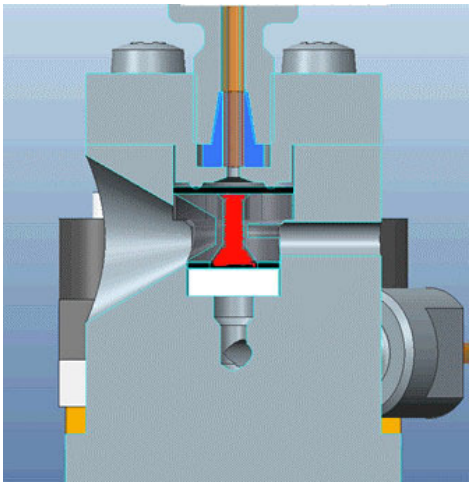

Figure 1.3: A sectional drawing of the osmotic pressure cell is shown. The sample volume is highlighted in red.

Another issue is the endurance of the osmotic pressure cell since the range of the pressure load should reach over several logarithmic orders from a pressure of 0.01 - 100 bar inside of the cell. Additionally, the cell is surrounded by vacuum during the measurement. The wide range of pressure is needed to cover the different regimes of intermolecular forces of the sample. However, the first prototype - a sectional drawing is shown in Fig. 1.3 - was designed for a maximum of 60 bar. The main reason to introduce a limit of 60 bar was to keep the cells polycarbonate

wall thickness low. Thinner walls provide better transmission of the x-ray beam.

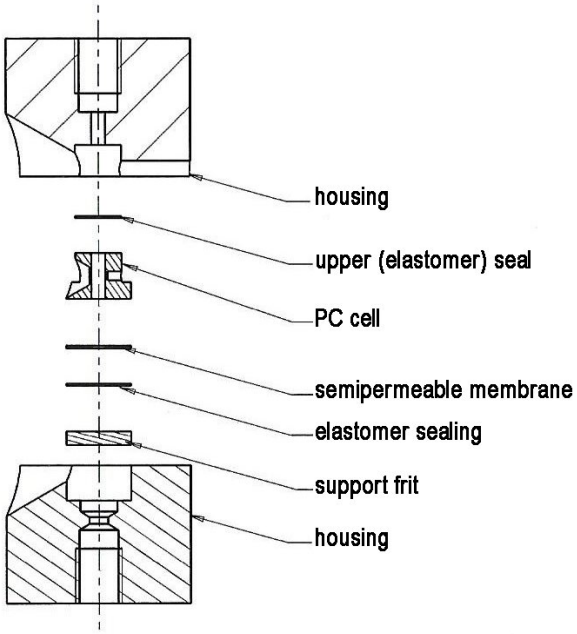

Figure 1.4: An explosion drawing of the main components of the osmotic pressure cell is shown.

For the cell itself polycarbonate was used as material with the thinnest part being the x-ray windows for incident and scattered beams (thickness: 1 mm). The whole polycarbonate cell is surrounded by a stainless steel housing which also connects the cell with the pressure applied through a hose from the top. On the bottom side an osmotic membrane separates the sample from the water reservoir. Both top and bottom sides are sealed by elastomer seals. Because of the high mechanical stress on the osmotic membrane a sintered bronze frit is needed as support. The alignment of these parts is shown in Fig. 1.4. In order to add movement in x-direction the OPC was mounted on the VarioStage for SAXSpace.

During experimental testing several changes to this setup were implemented which will be described more detailed in Sec. 2.

1.2.2 Pressure System

As already mentioned, an accurate pressure system is needed in order to perform such experiments. The main requirements for such a system are being able to maintain a constant pressure during the whole experiment and setting the pressure with an accuracy staying under the error tolerance. Previously Gauthé used water to transfer the pressure and apply it through a nonpermeable membrane to the sample. For this research compressed air is used instead, which is for several reasons superior. Firstly, the total costs can be kept lower.

Figure 1.5: Portable pressure setup for the osmotic pressure cell.

Furthermore, the elastic nonpermeable membrane can be skipped and pressure is directly applied to the sample. It is a crucial improvement since the elastic modulus of the nonpermeable membrane causes a back pressure. This back pressure leads to inaccuracies, especially when samples are measured in low pressure regimes. In case of high pressures the nonpermeable membrane has to deform and to penetrate deep into the sample chamber which also leads to pressure transfer loss due to geometrical constraints.

An overview of the pressure setup is shown in Fig. 1.5 with its main

components (A-F). In particular the pressure setup consists of a 200 bar compressed air cylinder (A) with a continuously variable 0 - 50 bar pressure regulator (B) and an analog primary pressure gauge (C). Since the analog secondary gauge (D) of this regulator exceeds tolerance for setting pressures below 20 bar, an additional digital 0 - 30 bar manometer (E) with an accuracy of 0.05 % full scale - which equals to 15 mbar - was mounted. Between the connection to the osmotic pressure cell a flow control (F) made by Anton Paar was installed in order to improve pressure circuit safety. PFA hoses were used to connect the pressure setup to the OPC using inverted cone joints on each side.

1.2.3 Experiment Preparation

To probe the properties and the functionality of the osmotic pressure cell lipid multilamellar vesicles (MLVs) were used as colloidal particles. In this particular case MLVs created with the phospholipid DOPC were chosen as dispersed phase and double distilled water was used as dispersion medium. Compared to other lipids DOPC is rather cheap and has a melting temperature at -17 °C [11]. Therefore, the sample stays always in the fluid lamellar phase in our test setup environment and additional complexity concerning phase transitions at laboratory temperature is avoided. MLVs preparation routine was performed as follows. Starting with thawing DOPC powder obtained from Avanti Polar Lipids (Alabaster, AL) and weighting-in the needed amount in a glass vial. After this, a lipid film is created by dissolving DOPC in chloroform-methanol (C:M 2:1) and evaporating the solvent using a Nitrogen stream for 10 min, followed by 24 hours of complete drying in a vacuum chamber. Finally the so created lipid film is rehydrated with 18 $M\Omega/cm^2$ water and is four times vortexed for 1 min every 15 min. After that the sample is ready to be loaded in the osmotic pressure cell. To measure osmotic pressure the excess amount of water in the sample needs to be as low as possible. Nevertheless, a too high DOPC concentration makes the sample gel-like and impossible to be loaded in the sample compartment of the osmotic pressure cell. By running many experiments - which will be discussed more closely in Sec. 2 - a sample with 33 w.t. % DOPC turned out working best for these

experiment needs.

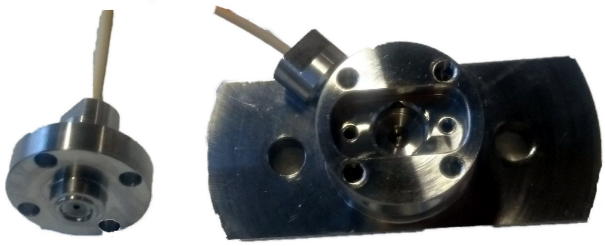

Figure 1.6: In this figure the upper (left side) and lower (right side) parts of the osmotic pressure cell housing are shown. The lower part contains two small threaded holes to screw the polycarbonate cell on the housing and four bigger threated holes to connect the upper with the lower housing part. The upper part is connected to the pressure system and the lower part to the atmospheric pressure in the lab using a high pressure hose.

Besides preparing the sample also the semipermeable membrane used in the osmotic pressure cell needs preparation. Membranes made of regenerated cellulose need to be washed and kept wet before using them in the cell. The created washing protocol consists of 10 min in 50 ml of EtOH (10 %) followed by two times 15 min in 100 ml purified water. Since membranes have the tendency to stick to the bottom or float on top, a magnetic stirrer with 300 rpm was used. After arranging the sample and the membrane, the osmotic pressure cell needs assembling to be ready for running an experiment afterwards. The first step is to place the support frit in the lower part of the housing (Fig. 1.6) and fill up everything with purified water. This will be the water reservoir in the osmotic process. Then the semipermeable membrane - which needs to be kept wet after the washing process - is placed on the frit. It is important that the membrane lies flat and centered on the support frit. On top of the membrane an O-ring with a diameter of 6 mm is placed. Again it is necessary to keep the membrane position in the center to avoid leakage of the sample.

Thereafter the polycarbonate cell is placed on top and fixed firmly with its two screws to the lower housing body. Before filling the sample into the measurement cell, the reaming excess water on upper side of the membrane and in the polycarbonate cell needs to be completely removed.

Figure 1.7: Components inside the housing are shown in original size. From left to right: housing screw, polycarbonate cell screw, cell side, cell top, bronze frit, O-ring, upper sealing with hole

Otherwise the leftover water dilutes the sample which leads to lower concentration and causes the experiment to fail. The upper sealing, which is a custom made elastomer square with a hole in its center, is placed on top of the polycarbonate cell. The sample should be filled from the bottom of the sample volume to the top using a pipette to prevent air bubbles in the sample column. Great caution is necessary to avoid touching the upper sealing, otherwise the sample can get sucked between the top surface of the polycarbonate cell and the sealing; and hence, the sample is lost. Finally the upper body of the housing is placed on top and kept in place by four firmly tightened screws (inner components are shown in Fig. 1.7). Now the osmotic pressure cell is ready to be mounted in SAXSpace.

1.3 Scientific Background

1.3.1 Intermolecular Forces

In nature there are four distinct forces known. Within the atomic nucleus strong and weak interactions take action. At atom and molecule scales, but also from subatomic range to infinity act electromagnetic and gravitational forces. Intermolecular interactions hold together condensed matter[12]. Their range and strength determine the matters macroscopic properties. All intermolecular interactions have their origin in the electrostatic force; however, it is convenient to distinguish between different types of interactions. Particularly interesting are bonds in the order of magnitude of thermal energy $k_B T$ [13].

Van der Waals Forces

Van der Waals forces arise from the interactions of neutral or charged atoms or molecules. These interactions are weak with an energy around the thermal energy at room temperature and long ranged compared to other intermolecular forces. The dissipation energy (U_{vdW}) between two atoms (molecules) is estimated with the polarisability α and their distance r as given in Eq. 1.1. In London theory this interactions are caused by instantaneously induced dipoles, in literature also referred as dipole fluctuations.

$$U_{vdW} \sim \frac{\alpha^2}{r^6} \tag{1.1}$$

Further contributions to the van der Waals forces are described by Debye forces which have their origin in a permanent dipole and its associated dipole. Keesom forces arise from permanent dipole interaction and also contribute to the net van der Waals forces. All three contributions to van der Waals interactions can be combined into a single theory, which takes into account the different propagation of electromagnetic waves in matter and is particular useful for manybody interactions occurring in general in condensed matter [13, 14].

Electrostatic Interactions

Ionic bonds are formed by electron transfer between the interacting atoms. Thereby created ions attract each other with the non-directional coulomb potential given in Eq.1.2 with the charges q_1 and q_2 at distance r and the electric permittivity in vacuum ϵ_0.

$$U_C = \frac{q_1 q_2}{4\pi\epsilon_0 r} \tag{1.2}$$

In general, ionic forces are stronger than van der Waals forces. However, in solutions the ions can freely move and screen each other which leads to exponential decaying coulomb interactions with distance. Further, van der

Waals forces act between all molecules, not just charged ones. Screened electrostatic forces have an interaction range comparable to van der Waals interactions, i.e. they may compete with each other [13].

Covalent Bonds

A covalent bond involves sharing of electrons between atoms. Through interacting with more than one nucleus the molecule's total energy is lower than the energy of the separated atoms. Covalent bonds are short ranged, highly directional and have energies much greater than $k_B T$ at room temperature. An example for covalent bonds is H_2 where sharing an electron pair allows both atoms to fill their outer shell. Common theories to explain the many kind of covalent bonds are valence band theory or molecular orbital theory [13, 15].

Hydrogen Bonding

A hydrogen bond is a special covalent bond between hydrogen and an electro negative atom such as oxygen or nitrogen. Since the hydrogen has only one electron for screening the protons coulomb potential, the opposite site to the electron has a high positive charge, which is able to interact with the electro negative atom. This leads to a bond which is weaker than regular covalent or ionic bonds, but stronger than van der Waals bonds. Intermolecular hydrogen bonding is responsible for the many peculiar properties of water [13].

Hydrophobic Interactions

Because of the fact that liquid water is forming a three-dimensional hydrogen bond network, other molecules perturb the local organization of water. In the case of nonpolar molecules, water forms a cage-like structure (clathrathes), leading to a decrease in entropy - which directly increases the free energy. If nonpolar molecules are brought closer together and fuse, the disturbing effect is reduced due to a decrease of the overall

surface area exposed to water. This leads to an attractive interaction which is known as hydrophobic interactions. In biological and non-biological system this interaction is a driving force for self-assembly [12, 13].

Steric Forces

Short interatomic distances lead to a strong repulsive force caused by the overlap of the atoms' electron clouds. This steric repulsion (also referred to as exchange repulsion) determines the smallest approachable distance between atoms or molecules and is very short in range. Using a hard sphere model for atoms, the repulsion force is steeply increasing at small separations and converging infinity. The van der Waals packing radius is also defined using the hard sphere model concerning steric forces and describes the packing of atoms or molecules [13].

Hydration Forces

Solvation forces, which consist of strongly monotonically repulsive, attractive and / or oscillatory forces, describe the interaction of solvent with solitudes. If water is the solvent, these short-range forces between atoms or molecules forces are called hydration forces and contribute to the stability of colloidal particles in aqueous solutions. Known effects are the spontaneously swelling of clay or lipid bilayers in water. Water molecules solvate solutes and ions because of the orientation of their dipole character and its resultant electrostatic interaction. This creates an orientational ordered hydration shell around the solute particles where especially the first layer is distinctive compared to bulk [13, 16].

DLVO Forces

The aggregation of colloidal particles in solution is quantitatively explained with the DLVO theory which is named after B. Derjaguin, L. Landau, E. Verwey and T. Overbeek. Based on the assumption that repulsion from electrostatic forces and the attraction from van der Waals

forces can be added, a total energy potential is calculated. The change of the potential with distance is shown in Fig. 1.8. The secondary minimum describes the equilibrium distance between particles / surfaces due to the addition of attractive and repulsive forces. Forces of entropic origin, such as steric repulsion between adjacent bilayers resulting from bending fluctuation, lead to a renormalization of all forces and consequently cannot be simply added to bare interactions in general [13].

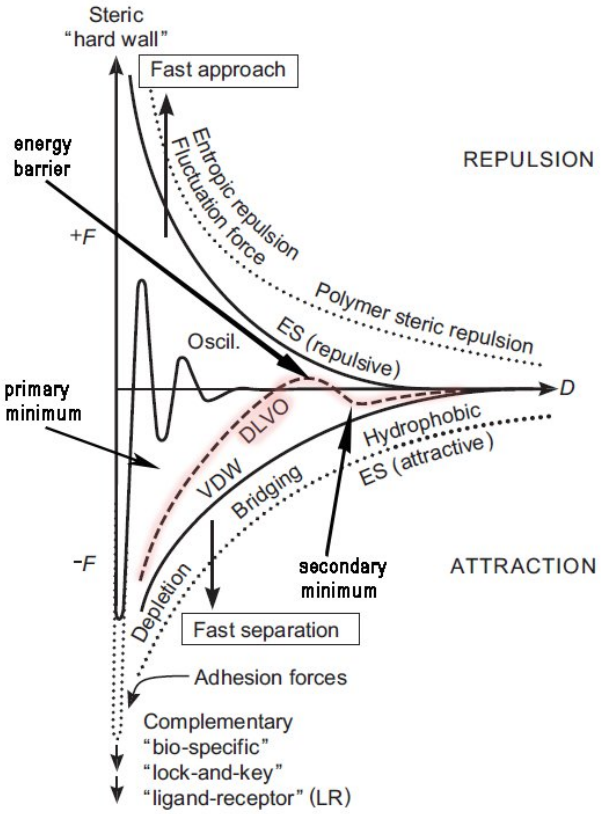

Figure 1.8: Addition of van der Waals and electrostatic forces leads to an attractive well at low distances which is also called primary minimum. The maximum, which lies in the repulsive force region, causes particles (if they can not overcome the energy barrier) to rebound after contact and therefore, the particles remain dispersed. In opposite to the first minimum, where particles aggregate irreversible due to its higher attractive force, in the secondary minimum the adhesion can be reversible. Adapted from [13]

1.3.2 Lipids

Lipids are small molecules with hydrophobic or amphiphilic properties and are soluble in nonpolar solvents. Lipids can form micelles, liposomes or other aggregates in aqueous solution because of their amphiphilic character [17]. For the experiment MLVs made of dioleoylphosphatidylcholine (DOPC) were used.

DOPC is a phospholipid with two unsaturated fatty acids (oleic acid 18:1) and a phosphatidylcholine headgroup linked with a glycerol backbone (Fig. 1.9). DOPC has a molecular weight of is 786 Da and is zwitterionic. This means DOPC has a neutral charge and lacks if hydrated with pure water, as in the present study, electrostatic interactions [18].

Figure 1.9: Structure of a DOPC molecule with hydrophobic tails and the hydrophilic headgroup. Figure adapted from [11]

1.3.3 Lipid Membranes

Biological membranes can be formed by lipids with different chain lengths, degrees of saturation, headgroup sizes, and charge where each of these specifications influences the properties of their self-assembly in aqueous solutions. Besides forming lamellar structures with fluid (L_α), gel (L_β,$L_{\beta'}$, $P_{\beta'}$) and subgel (L_c) phases, lipids are lyotropic liquid crystals, which means that they may display depending on their solvent (water/oil) a plethora of different aggregates, such as micelles, hexagonal or cubic phases. By the packing parameter $S = V_C / (A_h l_C)$ the formed structure

can be in many cases predicted using the ratio between lipid tails (V_C) and its area per headgroup (A_h) times the chain length (l_C) (S = 1 for lamellar phases). Multilamellar vesicles show an interlamellar spacing (d_w) which is determined by intermolecular forces. With the van der Waals interactions (f_{vdW}), the hydration forces (f_{hyd}), entropic interactions caused by thermal undulations of the bilayer (f_{und}) and electrostatic forces (f_{el}) in case of charged membranes an approximation of the interaction free energy per unit area (f) as a function of d_w and temperature is

$$\begin{aligned} f\left(d_W, T\right) &= f_{\mathrm{vdW}} + f_{\mathrm{hyd}} + f_{\mathrm{und}} + f_{\mathrm{elec}} \\ &= -\frac{H}{12\pi}\left(\frac{1}{d_W^2} - \frac{2}{\left(d_W+\delta\right)^2} + \frac{1}{\left(d_W+2\delta\right)^2}\right) \\ &\quad + P_h\lambda_h e^{-\frac{d_W}{\lambda_h}} + \left(\frac{k_B T}{2\pi}\right)^2 \frac{1}{\kappa} A_{fl} e^{\frac{-d_W}{\lambda_{fl}}} + f_{\mathrm{elec}}\,, \end{aligned} \tag{1.3}$$

with the Hamaker coefficient H, membrane thickness δ, hydration pressure constant P_h, hydration length λ_h, membrane bending rigidity κ, and membrane fluctuations parameters A_{fl} and λ_{fl} [18]. Disjoining pressures are simply given by $-\frac{\delta f}{\delta d_W}$.

1.3.4 Colloids

A colloid is a dispersion of insoluble particles or droplets in solution. Widely known colloids are milk, smoke or fog. The dimension of colloidal particles is ranging from 0.01 to 100 μm. In this range atomic properties make the transition to microscopic or macroscopic properties, and these properties are affected by molecular interactions. Colloidal particles can carry electrical charge which causes electrostatic interactions. The stability of a colloidal solution can be described by DLVO theory (Sec.1.3.1) [12, 13].

1.3.5 Small-Angle X-Ray Scattering (SAXS)

Small-angle x-ray scattering (SAXS) is a highly versatile technique for probing inhomogeneities of electron densities in matter found for example in minerals, complex molecules or biological structures. The x-ray diffraction formula Eq.1.4 shows that scattering angle Θ changes with the inverse of the distance between the lattice planes, which implies that for increasing lattices the scattering angle decreases.

$$\lambda = 2d \sin \Theta \tag{1.4}$$

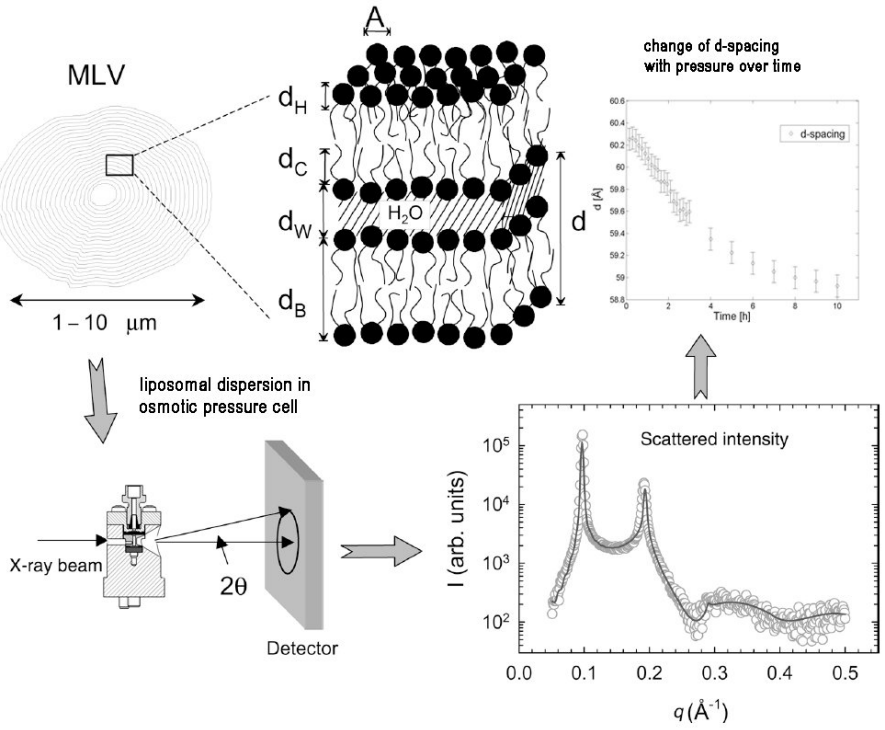

Figure 1.10: DOPC MLVs under osmotic pressure are exposed to the x-ray beam and the scattering intensity I as function of the scattering vector q is recorded. By repeating this measurement the change of the d-spacing over time can be obtained. Adapted from [19].

SAXS is a non-destructive measurement method to gain averaged structural informations, but no local structure details. In the case of lipid MLVs, the bilayers lamellar repeat distance can be obtained with Eq. 1.5. In Fig. 1.10 the principal of a SAXS experiment to measure bilayers lamellar repeat distance and its change with pressure over time is shown [20, 21].

$$d = \frac{2 * \pi * n_{order}}{q_{peak}} \tag{1.5}$$

1.3.6 Osmotic Pressure Applications

In the osmotic pressure technique the pressure between colloidal particles such as clay sheets, lipid bilayers and biological macromolecules is measured. A commonly used approach is to introduce osmotic stress large neutral polymers, which do not interact with the material and which are large enough to be excluded from the interstitial water layers. Adding an osmolyte of known osmotic pressure (e.g. polyethylene glycol (PEG)) to the colloid is an easy and cheap way to set an osmotic equilibrium at known pressure. In the case of MLVs in water PEG competes with the lipid for available water which leads to a decrease of the water layer between the lipid bilayers. However, this technique requires a new sample for every osmotic pressure, takes days for equilibration time and is difficult to use for high pressures due to its high viscosity. Additionally, the scattering intensity originating from the polymers increasingly overwhelms with concentration contributions from MLVs [9, 22]. Another way to apply osmotic pressure is a cell with a semipermeable membrane which divides the colloid from a solvent reservoir. A known physical pressure squeezes the excess dispersion medium through the pores of the semipermeable membrane until the osmotic pressure equilibrium is reached. The advantages of this technique are that only one sample is needed for various pressures and that the process is reversible.

The osmomanometer [8] describes a setup using manometrical imposed pressure (Fig. 1.11). The upper sample container with the colloids is separated by a semipermeable membrane from the lower compartment which is connected to its solvent reservoir using a column. Both the upper

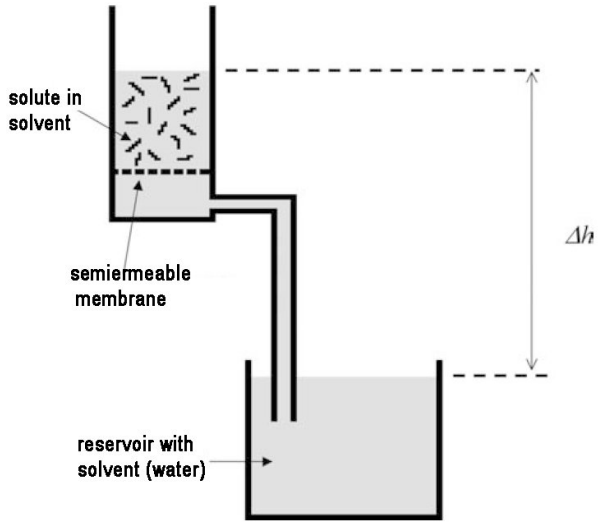

Figure 1.11: Shown is the osmomanometer using height difference between the colloid and the reservoir with the solvent to create an osmotic pressure. The solvent is permeable through the semipermeable membrane, but the solitudes are held back. An advantage of this setup is that there is no calibration of the absolute pressure necessary. Adapted from [8]

compartment with the solute and the solvent reservoir at the bottom are exposed to atmospheric pressure. Therefore, the osmotic pressure is only defined by the height difference as given in the hydrostatic formula $p = \rho g \Delta h$ with solvent density ρ and gravity g. Since Δh of 1 m equals to 0.1 bar, this setup is not feasible for high osmotic pressures.

Further development based on principles of the osmomanometer was achieved by [9]. The upper and lower compartments were combined in one cell and divided by a regenerated cellulose dialysis membrane supported by a porous steel frit. The pressure was now applied by compressed water via an elastic nonpermeable membrane from the top. The sample volume was reduced to 25 µl and surrounded with a temperature controlled environment. Their aim was to measure the osmotic pressure ranging from 0.1 - 100 bar with only one sample. The sample consisted of DOPC MLVs and the lamellar repeat distance was measured with SAXS.

1.3.7 Semipermeable Membranes

The reverse osmosis process in osmotic pressure cell uses semipermeable membranes with selective diffusion of molecules based on their size. For this special purpose are no membranes manufactured; however, membranes made for dialysis or ultrafiltration have similar properties. To find the right membrane several parameters like pore size, flow rate or deformation under pressure have to be taken account of. Used dimensions for pore sizes in ultrafiltration are molecular weight cut off (MWCO) relating to the 3-dimensional molecular size or metric length regarding to the pore size diameter (Fig. 1.12). Especially in the case of lipid MLVs with a size from 50 nm - 1µm (>700 kDa) high pressure can lead to extrusion if the pore size is chosen too big [23]. For dialysis membranes Spectra Labs recommends a MWCO which is a tenth of the regarding solitude size.

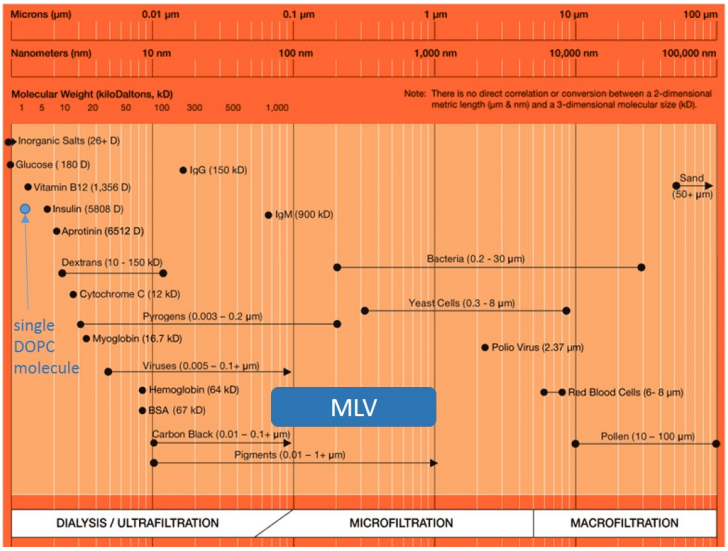

Figure 1.12: Relations between pore diameter and MWCO are shown in this pore size chart. Adapted from [24]

Semipermeable membranes are starting from 100 - 500 Da and hydrophobic or hydrophilic surfaces are available. Because divers materials are used, best working pretreatments have to be found in each case.

Cellulose Membranes

For dialysis application cellulose membranes are most commonly used. Regenerated Cellulose (RC) and Cellulose Esther (CE) membranes are almost same. The difference is that RC membranes get an additional treatment which provides superior temperature tolerances and chemical compatibilities. These membranes are ranging from 100 - 1,000,000 Da and are available in different qualities. Usually cellulose membranes are packed with glycerin which needs to be washed off before usage. Advantages are the high mechanical strength and low cost. The biggest disadvantage is the material consistency which leads to various flow rates.

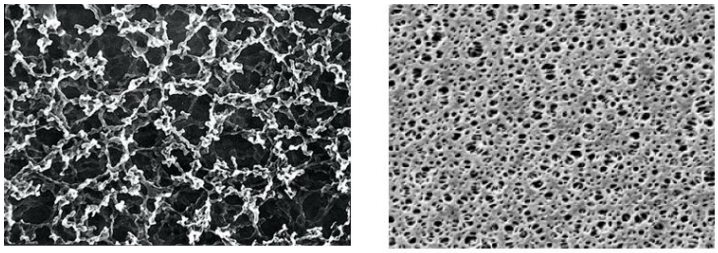

Figure 1.13: On the left side the structure of a RC membrane is shown. The small pore size is achieved with stacked layers of polymer rods. A track-etched PES membrane's structure with straight pores is shown on the right side. Adapted from [25, 26]

Polycarbonate / Polyethersulfone Membranes

Although thermoplastic membranes are mainly used for extrusion, small pores sizes (>5000 MWCO) are available. This track-etched membranes have sharply defined pore sizes and a higher flow rate compared to cellulose membranes. A drawback is that malfunctions occurred at high pressures during our experiments such as sudden loss of sample probably caused by enlarged or broken pores. A comparison of the structure of a cellulose membrane from Sigma-Aldrich Handels GmbH (Vienna, AT) and the structure of a polyethersulfone polyethersulfone (PES) membrane

from Altmann Analytik GmbH & Co. KG (Munich, DE) is shown in Fig. 1.13.

Anodic Aluminum Oxide Membranes

During the experiment nanoporous alumina membranes with 20 nm and 25 nm from SmartMembranes were tested. Because of their high pore to surface ratio the flow rate of this membranes is superior to others. Also their thickness with only 50 - 60 µm contributes to the high flow rate. Because of their thickness and brittle material the tested membranes were very prone to cracks and long run measurements were impossible. The main problem was the force from the O-ring at the edge of the membrane discs. From the quality assurance of SmartMembranes (Halle (Saale), DE) EM images of the used membranes were provided as shown in Fig. 1.14.

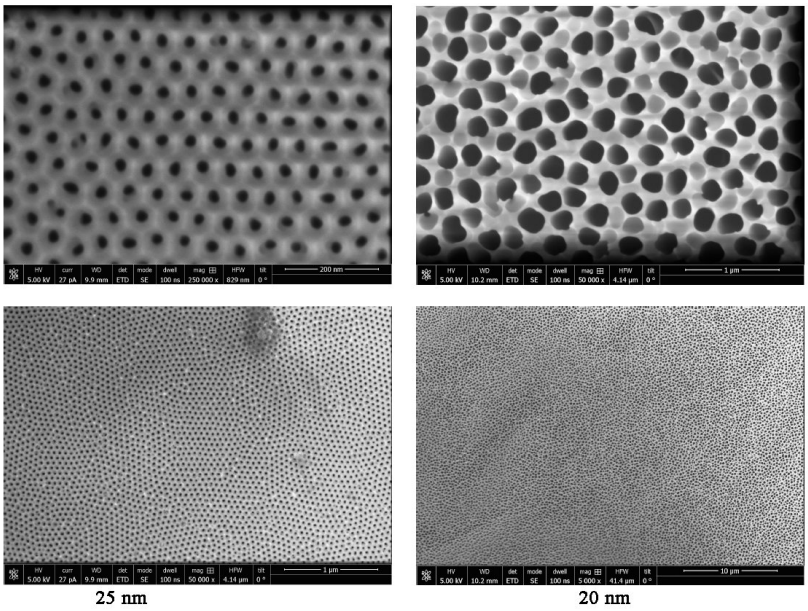

Figure 1.14: At the left side SmartPor EM images are shown. The pores are highly ordered with a diameter of 25 nm which stays constant through the length of the pore. At the right EM images of FlexPor membrane with 20 nm pore diameter is shown. Because of the lower order the pore to surfaced ratio is increased and the flow rate is higher.

2 Experiment and Development

Although the theory behind the setup - which was described in Sec. 1.2 - is straightforward, running the experiment turned out to be quite challenging. Also since there are only a few setup approaches for applying osmotic stress on a sample by using a pressure, not many parameters were known at the beginning. Understanding how the variability of single components like the permeable membrane material, its pore size and its flow rate and the change of these parameters in different pressure regimes, required various test runs and adaptations as described in the following sections.

2.1 Performing an Experiment

Every experiment starts by preparing the sample, treating the semipermeable membrane and loading the sample into the osmotic pressure cell as described in Sec. 1.2.3. After that the osmotic pressure cell is mounted in the SAXSpace using the VarioStage and connected to the pressure system. The sample detector distance (SDD) was set 307.5 mm for all experiments. To prove the functionality of the osmotic pressure cell, the change of the lamellar repeat distance of DOPC MLVs was measured. Usually one reference measurement is taken at 0 bar. Thereafter the desired pressure is set and the d-value is measured in chosen time intervals as described in Sec. 2.1.1. Since more than 100 experiments were performed, only major insights and their consequential changes are presented in Sec. 2.1.2.

2.1.1 Determining the d-Value using SAXS

Exposure times starting from 30 seconds (depending on the sample concentration) are sufficient to obtain a scattering pattern as shown in Fig. 2.1 and determine the d-spacing of a sample.

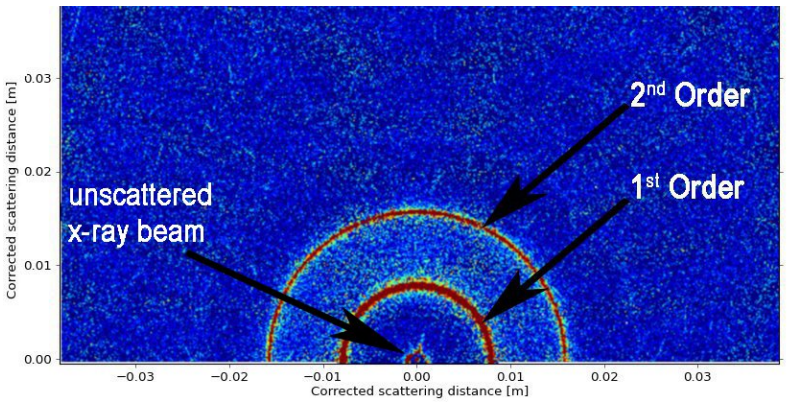

Figure 2.1: A typical SAXS scattering pattern for DOPC is shown. The inner and outer red circles are the first and second order, respectively. This picture was obtained with SAXSpace using a DOPC probe

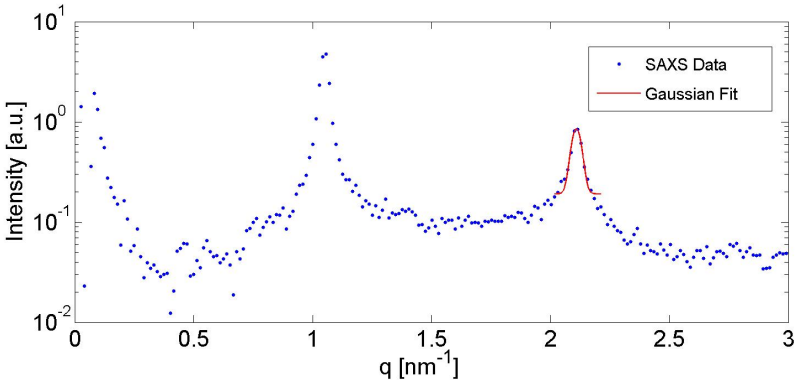

Figure 2.2: SAXS pattern from a single SAXS measurement already processed and imported to MATLAB. The position of the second order peak is determined by fitting a Gaussian distribution (red line) and used to calculate the d-value.

By angular integration over the scattering pattern intensities using the SAXSanalysis software, a 1D plot of ”q vs. I” is calculated. From the

maximum of any order and the corresponding q-value, the bilayers d-spacing can be calculated with Eq. 1.5. In case of short exposure times, the second order was used for the calculations since the accuracy is better than using the first order and the intensities of higher orders lie in the noise.

Equilibration of the sample at a given osmotic pressure was followed by time-resolved SAXS with varying time intervals with high enough resolution to track the change with pressure. Next a MATLAB script (see Appendix) was used to find the d-value for every single measurement as shown in Fig. 2.2. Another MATLAB routine was used to plot the evolution of d with time (Fig. 2.3). These basic steps were performed repeatedly to find the best setup (e.g., membrane, sample concentration, sealing, etc.).

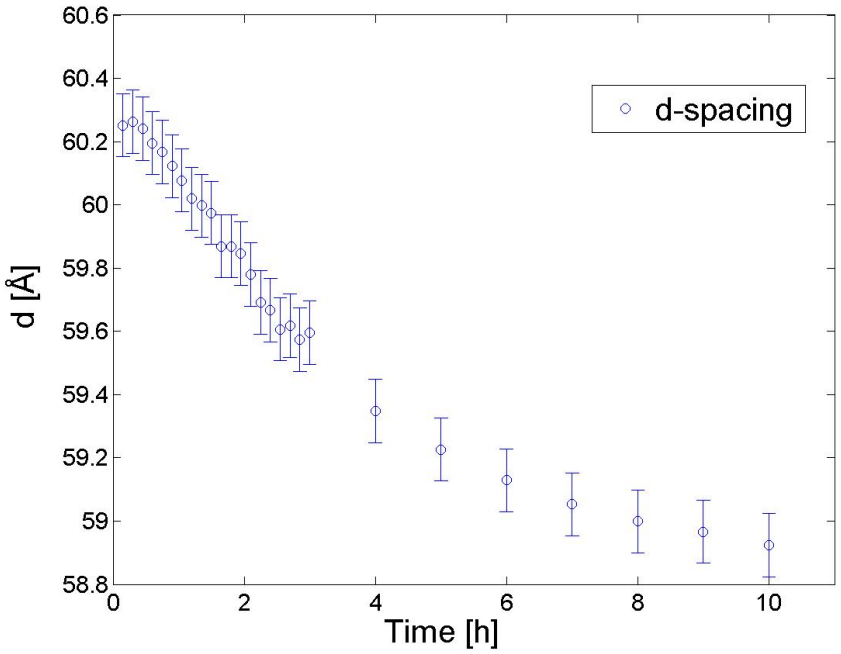

Figure 2.3: Equilibration of DOPC MLVs at an osmotic pressure of 1 bar over a period of 10 hours. The initial sampling rate was set to 15 min and extended to 1 h after 3 hours. The used RC membrane MWCO was 100 kDa.

2.1.2 Setup Problems and Improvements

During preparing, executing and evaluating experiments, several issues appeared. Following essential improvements are listed chronological.

Upper Sealing and Support Frit

After the first test runs, it turned out that height of the used steal support frit was too low and the cell was not leak-proof under pressure. Therefore, it was replaced with a slightly thicker brass frit. Due to this change there was higher compression on the O-ring and no more leakage occurred. Another advancement was to introduce a hole in the upper sealing, which was only an elastomer square at the beginning. Since the pressurized air has no effects on the sample, problems with the pressure transfer through the membrane can be avoided by adding a hole to the upper sealing and the back pressure of the elastic nonpermeable membrane has no more influence on the experiment. Furthermore, it was possible to load more sample, which was important, since the first measurements were performed at lower DOPC concentrations.

Temperature Fluctuations

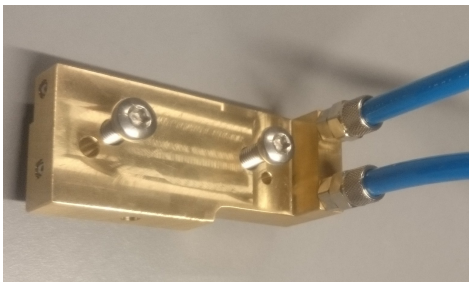

Figure 2.4: Water cooling for thermal isolation of the osmotic pressure cell from the VarioStage. The brass body of the cooling is bolt-on the VarioStage and connected to a water cooling pump with quick connectors.

After the sealing was capable of running longer experiments, the heat transfer from the sample stage (from electrical motor which keeps the sample in place) turned out to be a problem for measurements. Thermal energies are in the same energy region as intermolecular forces, hence a constant sample temperature was needed. The solution for this problem was a water cooling between the VarioStage and the osmotic pressure cell shown in Fig. 2.4.

Semipermeable Membranes

With ongoing experiments and improvements the biggest issues were finding the right membrane and its pretreatment. In Sec.1.3.7 the different types of membranes which were studied and their advantages and disadvantages were discussed. However, it took several tries to find the proper membranes. The first experiments were performed without membrane preparation, and therefore failed to supply successful and reproducible results. The answer to this problem was a proper pretreatment as described in Sec. 1.2.3. Also compromises regarding the pore size had to be made. Whereas big pores provide higher flow rate, their size is limited since the extrusion pressure is proportional to the inverse of the pore size [23]. This implies that the vesicles can penetrate through the semipermeable membranes at certain pore size /pressure ratios. Furthermore, the structure of the membrane itself may change due to the high pressure in the cell and can show different behaviors over the pressure regions. The maximum recommended pressure for cellulose membranes is 1.5 psi in the Spectrum Labs RC membranes manual. Generally, a big issue is the variation of the membranes itself even for nominally equal products. For example, RC membranes are punched out of a dialysis membrane. Because of the bigger surface in dialysis processes, disparities have no negative effect, whereas using it as a filter in an osmotic pressure experiment a poor membrane can change to outcome of the whole experiment.

Redesign of the Osmotic Pressure Cell

It turned out that the x-ray beam was to far away from the surface of the semipermeable membrane for the first OPC version. In particular the osmotic pressure induced compression of concentrated the sample below the transmitting x-ray beam, consequently precluding any determination of its d-value. There were two ideas to fix this issue. The changes of the OPC dimensions are marked (A-E) in Fig. 2.5.

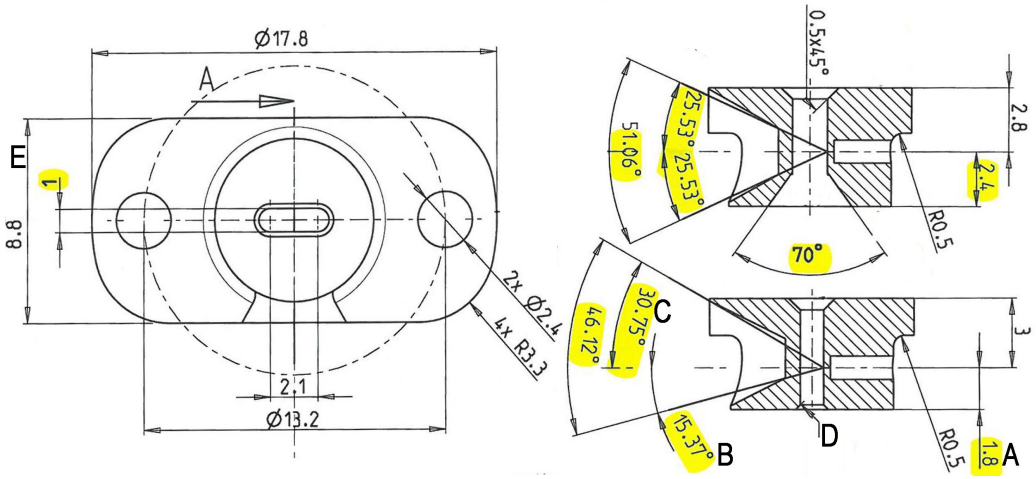

Figure 2.5: On the left side is a top view of the second OPC version. On the upper right side a sectional drawing of the first OPC version is shown and below is a sectional drawing of the new OPC version. Important dimensional adaptations are highlighted.

First the x-ray windows of the inner polycarbonate cell were lowered by 25% from 2.4 mm to 1.8mm (A). This change effected the negative angle of reflection (B); however, only the positive angle of reflection(C) - the 2Θ-angle - is used in SAXS. The second major change was removing the inside cone at the bottom of the polycarbonate cell and add a small bevel instead (D). This cone had no use because of the low flow rate. Also pressure in liquids applies in all directions.

These changes lowered the relative sample volume beneath the x-ray beam and increased the amount above the beam. Additionally, the width of the sample container in beam direction was decreased from 1.5 mm to 1 mm (E). Altogether, all changes added up to $\sim$ 43 % reduction of the sample volume to with a significant higher percentage of compressed sample above the x-ray beam.

Further Optimizations

In order to improve the connection with the water reservoir we added a support filter between the bronze support frit and the semipermeable membrane. Furthermore, a small sphere was placed underneath the semipermeable membrane to increase the interacting surface. For better sealing at high pressures the thickness of the upper elastomer seal was doubled. Because of this the excess material got pushed towards the center hole and sealed it completely in some cases, hence material at the outer corners of the upper seal was removed.

3 Results and Outlook

3.1 Osmotic Pressure Cell: Version 1

To figure out usage and properties of the OPC (mounted on the VarioStage) measurements were performed using different DOPC concentration without pressure (Fig. 3.1). Also 18 MΩ/cm² water was measured which is needed to subtract the sample's background. The used detector was Dectris Pilatus 100K-S.

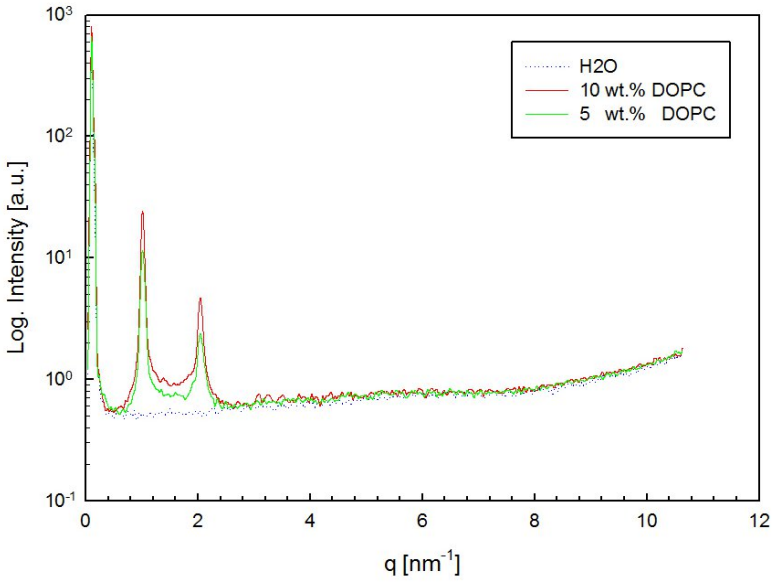

Figure 3.1: Intensity rises with higher sample concentration, whereas d-spacing stays the same. The H_2O sample is used as background measurement originating from water and OPC. For each sample the exposure time was 3 times 10 minutes at 0 bar.

The transmission of the OPC was compared to the μCell (quartz capillary) to obtain further performance information (Fig. 3.2). Although the intensity measured with the OPC was slightly lower, the first and the second order are significantly above the noise and the d-spacing of DOPC can be calculated using the peak maxima, see Sec. 2.1.1.

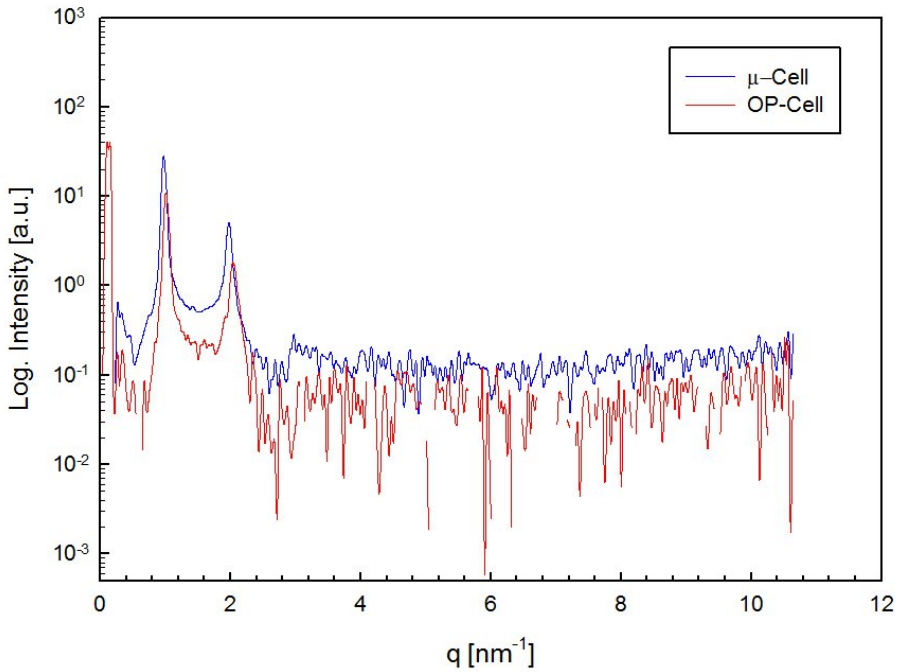

Figure 3.2: Comparison of scattering signal of OPC and μCell with subtracted backgrounds. The used sample was DOPC (5 wt.%) with 3 times 10 minutes exposure time.

The next step was checking the seal tightness. In Fig. 3.3 is shown that the OPC remained tight under vacuum for 68 hours; however, an increase in d-spacing and a decrease in intensity was detected caused by change of sample temperature. The origin of the heat was the VarioStage, see Sec. 2.1.2. From now on water cooling was used for further experiments.

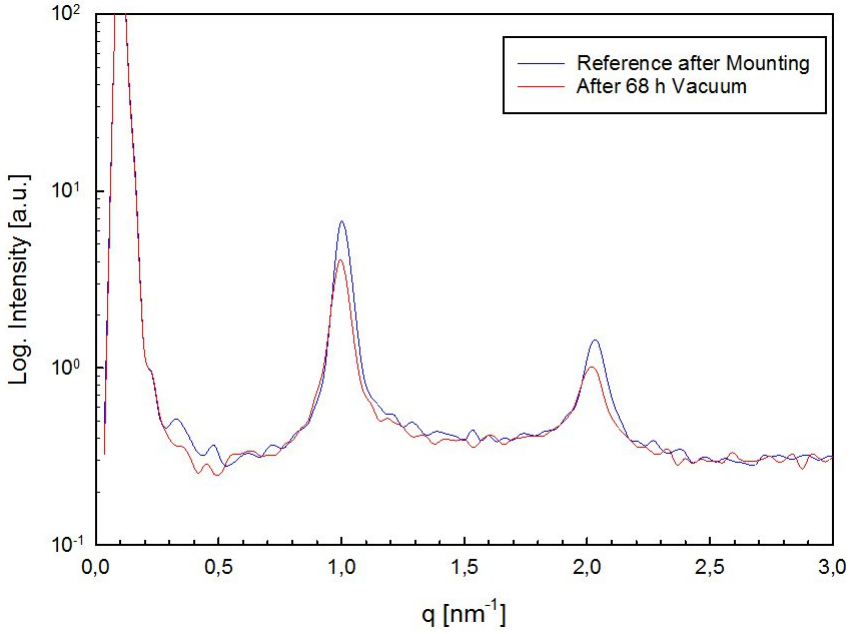

Figure 3.3: The change caused by temperature shows that thermal energies strongly influence intermolecular forces. Constant sample temperature is required for further measurements.

For future evaluation, an osmotic pressure calibration curve using the osmotic stress technique with PEG 8000 [27] was measured and compared to reference data (Fig. 3.4). In case of high pressure this method is limited due to the PEG 8000 viscosity. Deviation from the reference may caused by short sample equilibrium time.

Simultaneously with the water cooling also an Eiger R 1M detector, which provides higher resolution, was installed and used from that moment. An early experiment with a 20 kDa RC membrane using 20 wt. % DOPC at 1 bar and 20 bar showed no significant change in d-spacing over a period of 22 hours. The flow rate of the used membrane was to low which maybe caused by blocked membrane pores as shown in Fig. 3.5 and poor initial flow rate through the membrane. This experiment also pointed out that the membrane's flow rate is one of the major limiting factors concerning osmotic pressure equilibration time, hence alternative semipermeable membranes were tested.

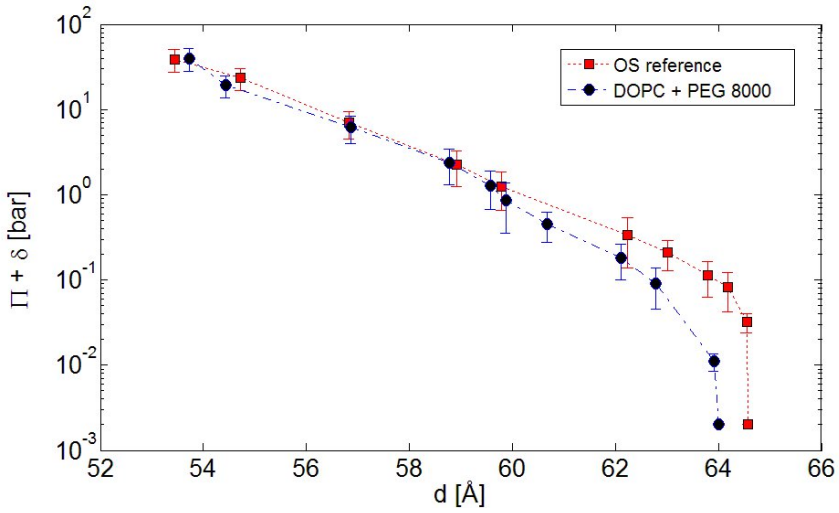

Figure 3.4: Change of DOPC MLVs d-spacing with pressure using osmotic stress (PEG 8000). Data point at 64 Å represents pure DOPC. An offset of $\delta = 2 * 10^{-3}$ bar is added to the OS data for logarithmic plotting. Reference taken from [28]

To improve the flow rate the next experiment was executed with a 100 kDa RC membrane. Because of the new membrane with its bigger pore size, first proof of the OPC functionality could be achieved measuring a change of d-spacing of more than 1 Å, see Fig. 3.6. On the downside, the sample sank under the x-ray beam before reaching its osmotic equilibrium state. Possible reasons were low sample concentration (too much water within the sample) and loss of DOPC through the pores or leakage during the experiment.

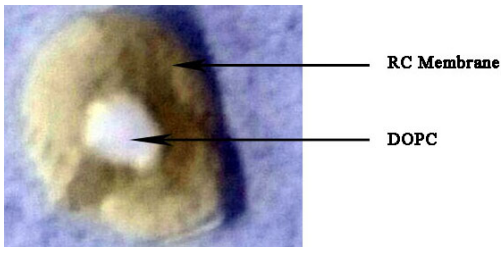

Figure 3.5: RC membrane after experiment. The white DOPC MLVs are blocking the membrane pores and cause lower flow rate. This effect can lead to a gradient within the sample towards the semipermeable membrane.

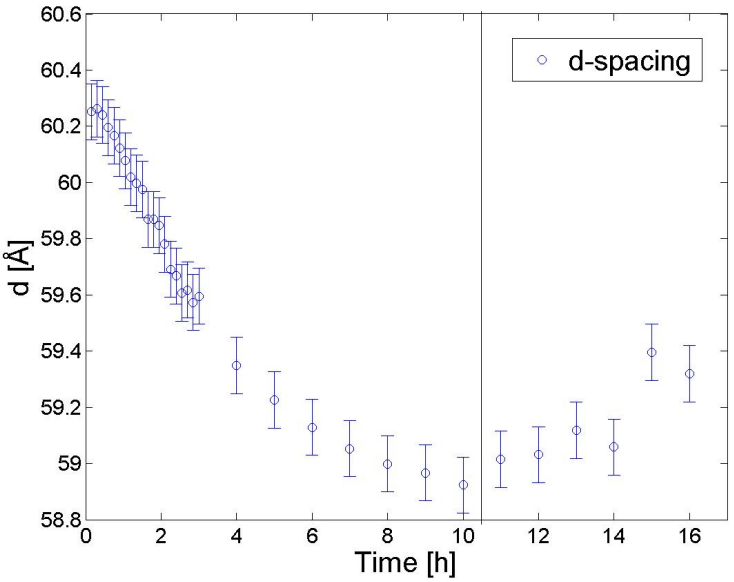

Figure 3.6: An experiment with 100 kDa RC membrane at 1 bar, 20 wt. % DOPC. After 20 measurements the time interval was extended from 9 min to 60 min. D-spacing after 10 hours was 58.9 $\pm$ 0.1 Å. Before the equilibrium was reached, sample sank below x-ray window (after 10 hours). Besides the deviation from the trend, the last five scattering patterns had very low intensities (only leftover sample on the cell wall).

Several semipermeable membranes were tested in order to find the best for the OPC. Polycarbonate membranes (15 and 50 nm pore size) showed low flow rate and fast sample loss after overcoming certain pressures (>4 bar). Similar characteristics were observed using a PES membrane (5 kDa MWCO) with low flow rate and sample loss at pressures >10 bar. High flow rates were obtained using aluminum oxide membranes (20 and 25 nm pore size), but the fragility and difficult handling of these membranes made them unsuitable for long experiments, see Fig. 3.7.

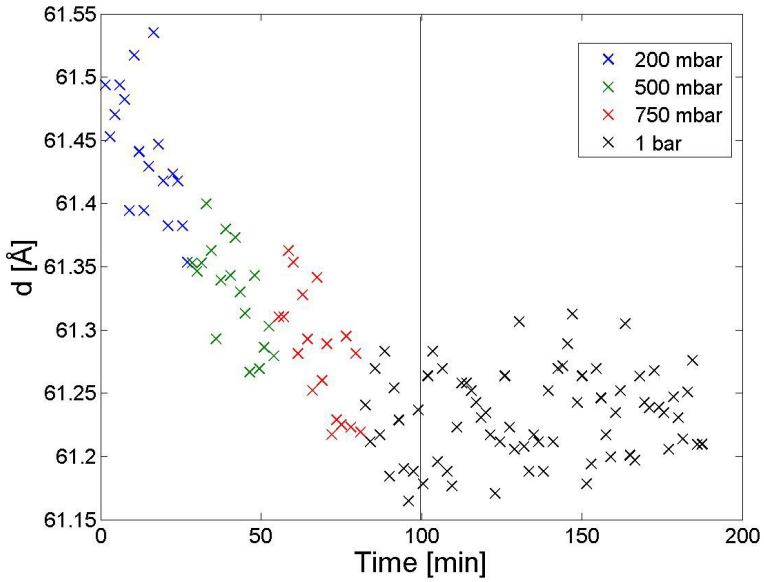

Figure 3.7: Example of a pressure ramp experiment for analyzing membrane properties using a 20 nm anodic aluminum oxide membrane. Through the high flow rate change of d-spacing occurred immediately, but due to cracks (discovered after disassembling the OPC) sample was lost after 100 min. D-values after that time are based on remaining sample on the cell walls. The sample loss can be approved by lower scattering intensities.

Next, CE membranes with pore sizes of 0.1-0.5 kDa, 0.5-1.0 kDa, 3.5-5 kDa, 8-10 kDa, 20 kDa, 50 kDa and 100 kDa MWCO and RC membranes with 3.5-5 kDa, 8-10 kDa, 14,5 kDa, 20 kDa and 100 kDa MWCO were tested using the preparation protocol described in Sec. 1.2.3. As a result of these tests, the Spectrum Biotech 100 kDa MWCO CE membrane turned out to perform well at low pressures and the Spectrum Spectra/Por 3.5-5 kDa MWCO RC membrane at high pressures (>5 bar).

After the right set of membranes was found, further experiments showed that the geometrical dimensions of the OPC prohibited measuring higher pressure. However, the upper levels of the sample always ended up below the x-ray window, even at high sample concentrations, which led us to the modifications of the OPC (Sec. 2.1.2).

3.2 Osmotic Pressure Cell: Version 2

The first experiment with the OPC version 2 was performed using a 100 kDa MWCO CE membrane. This experiment pointed out the variation of cellulose based membranes even within nominally equal types; and with the ongoing experiment the pressure was increased (Fig. 3.8) in order to unblock pores and raise flow rate. Again, sample was lost before reaching equilibrium and it was hard to determine the cause of sample loss. However, membrane failure or leakage were highly likely.

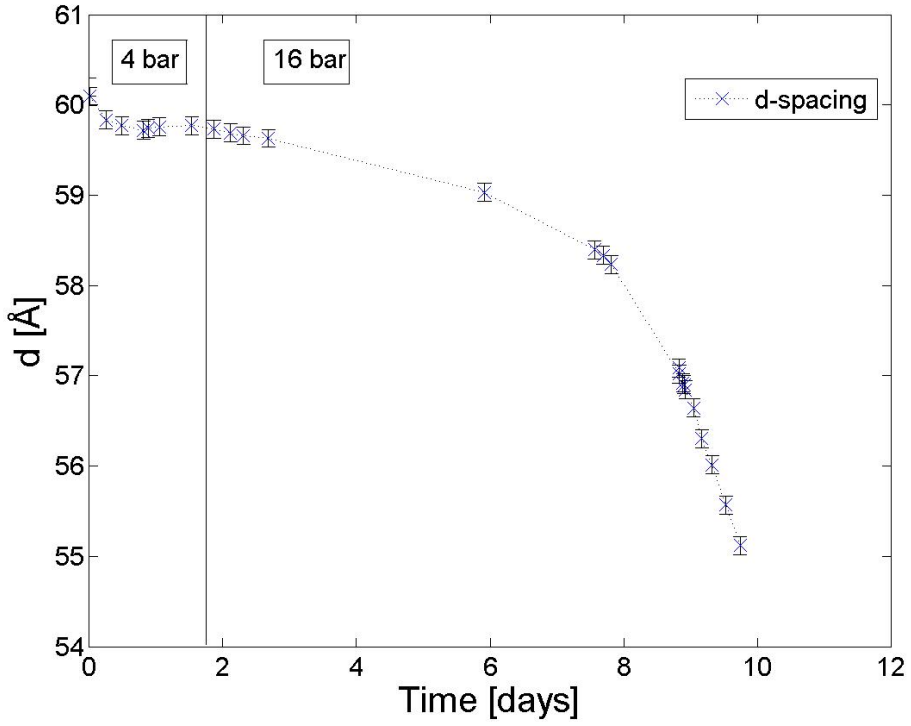

Figure 3.8: After two days the pressure was raised to 16 bar. Before reaching osmotic equilibrium sample was lost. The flow rate at low pressures was low compared to other measurements with a 100 kDa MWCO CE membrane which indicates variation within the same type of membrane.

In order to examine higher pressures the 3.5-5 kDa MWCO RC membrane was installed and a 20 bar equilibrium was reached. Thereby the function of OPC version 2 was proven. As shown in Fig. 3.9, it took almost two days before a change in d-spacing took place. This could be caused by dehydration starting at the membrane's surface. Gradient experiments after equilibrium was reached and during rehydration showed coexisting phases and distinct local order depending on the distance from the membrane (Fig. 3.10).

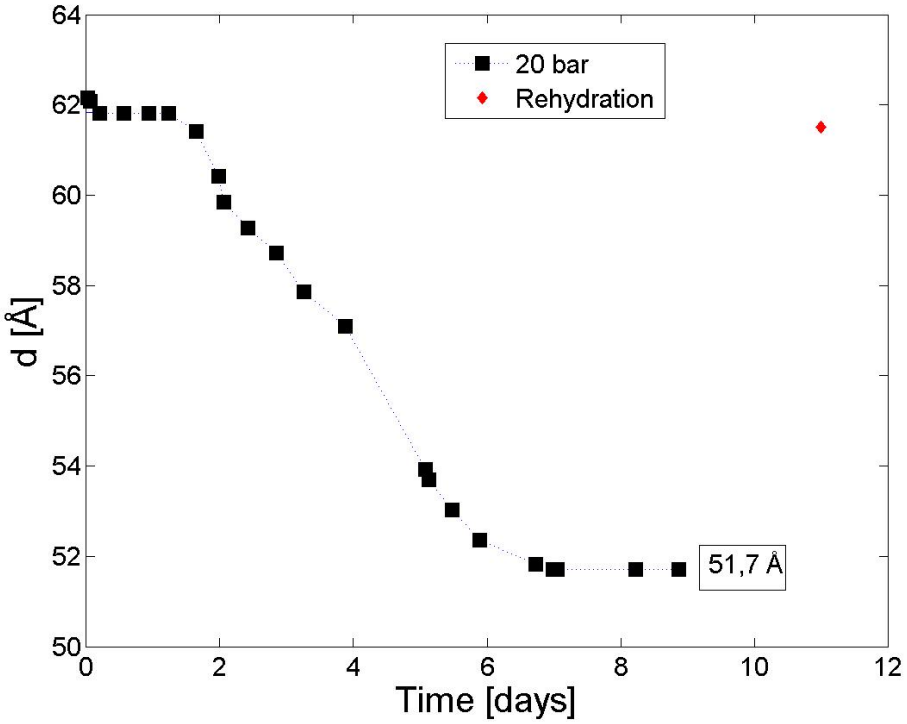

Figure 3.9: At 20 bar osmotic pressure equilibrium (51,7 Å) was reached by using a 3.5-5 kDa RC membrane. Also rehydration (61,5 Åat 0 bar) of the sample within 3 days was accomplished. Detector problems caused loss of data points in this experiment. Measurement errors lie within marker size.

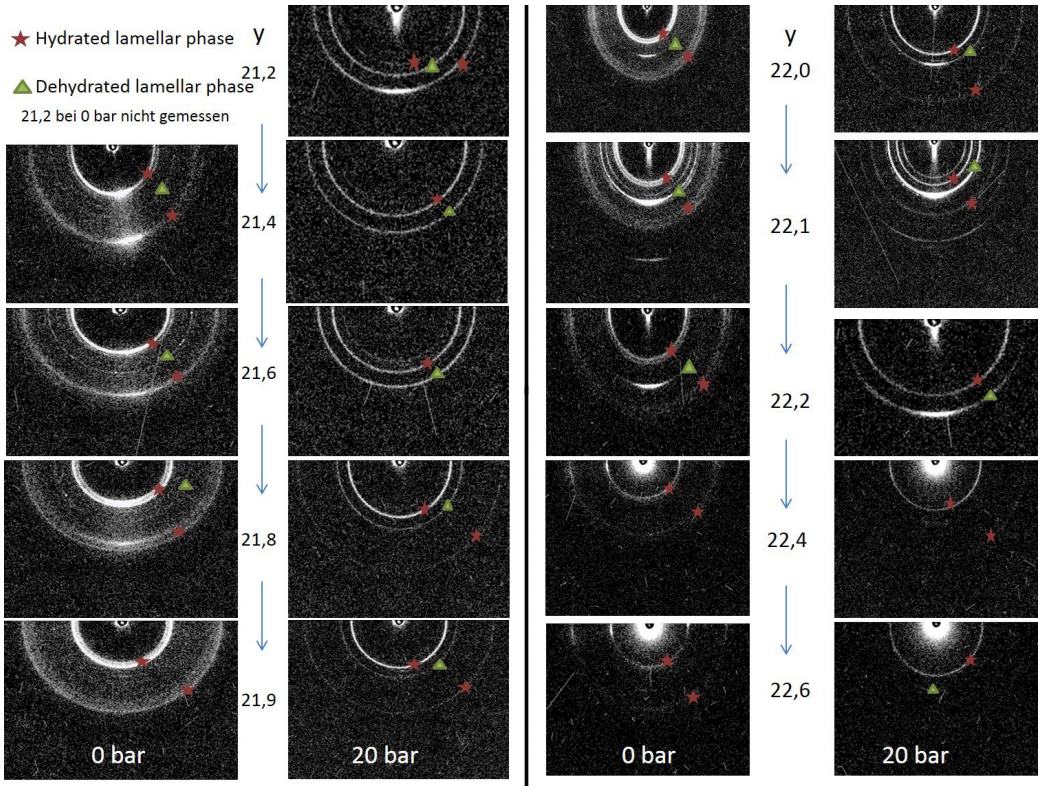

Figure 3.10: Gradients after 20 bar equilibrium and during rehydration. In both cases local orientation was observed. During the rehydration process coexisting hydrated and dehydrated lamellar phases occurred. The position of the OPC with respect to the x-ray beam is given by y. That is in increase of y means that x-rays probe the sample closer to the semipermeable membrane.

An experiment at 7 bar (Fig. 3.11 confirmed the functionality as previously observed in the 20 bar experiment. During this experiment sample loss occurred during the rehydration process caused by leakage of the upper seal (first from right in Fig. 1.7). Since this seal was adapted from previous test runs, a new design of the seal, as suggested in Sec.3.4.1, would be beneficial to future measurements. During the whole experiment no gradient was detectable in the sample which shows that the hydration and dehydration processes are not fully understood yet.

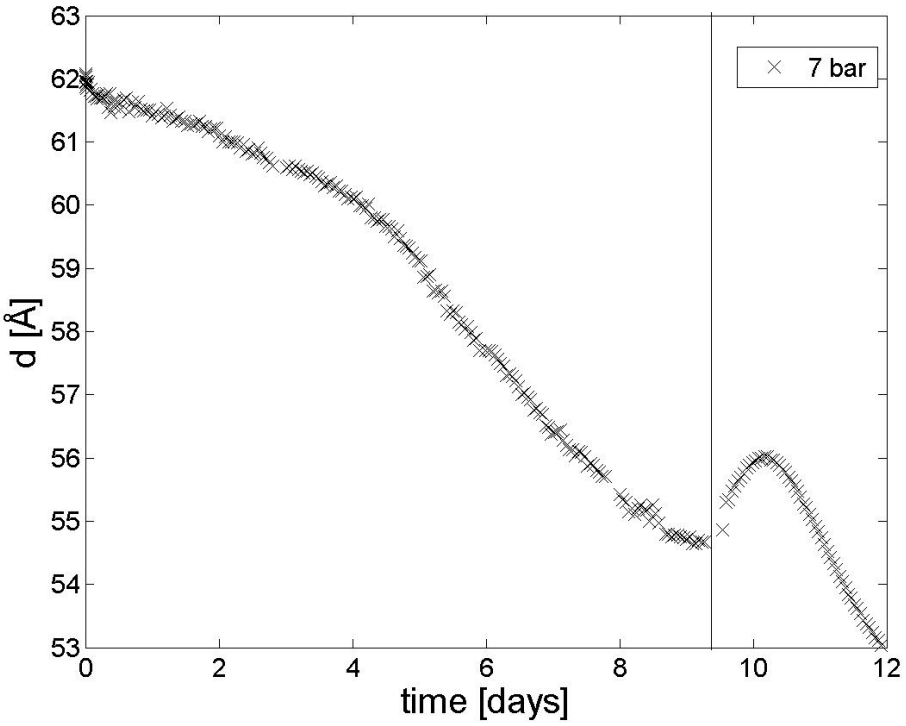

Figure 3.11: For higher resolution this experiment was performed with a time interval of 30 min and equilibrium reached at 54.5 Å after 224 hours. Rehydration worked well until sample was lost after 10.3 hours, due to malfunction of the elastomer seal. The followed decrease of d-spacing is caused by drying out of the sample under vacuum and only remains at the cell walls are measured. This is detected by changing scattering patterns intensities. Measurement errors lie within marker size.

3.3 Final Result

Equilibrium data of the OPC experiments are compared to the reference data from the OS technique with PEG 8000 in Fig. 3.12. Furthermore, an advantage of OPC over OS is a smaller measurement error.

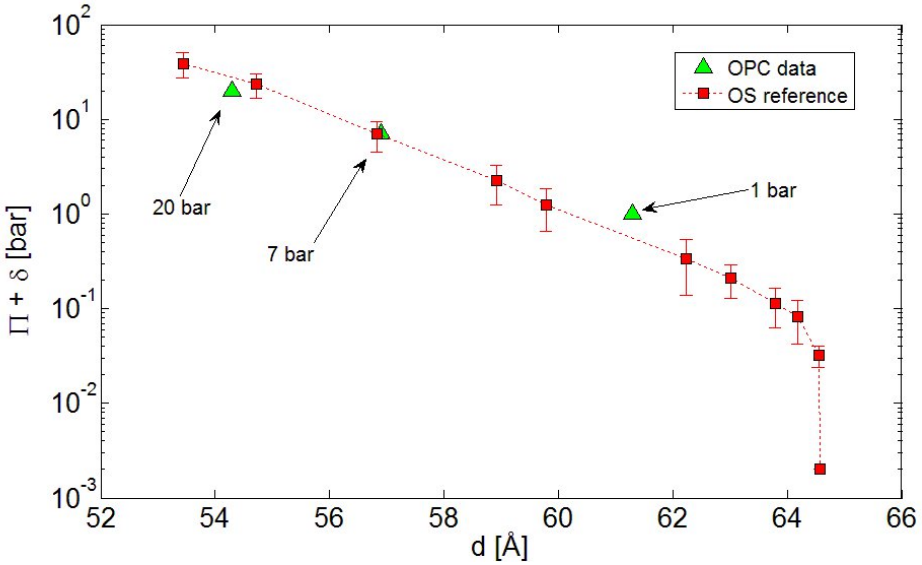

Figure 3.12: In order to compare the OS method with the OPC method the d-values obtained with the OPC were shifted by 2.4 Å. This equals to their difference at 0 bar caused by measuring with different setups (see Fig. 3.2). In two cases (7 and 20 bar) osmotic equilibrium was reached using the OPC and it agrees with the results from osmotic stress [28]. Also the 1 bar data fits, since equilibrium state was not completely reached and a shift to lower d-spacing is expected. An offset of $\delta = 2 * 10^{-3}$ bar is added to the OS data for logarithmic plotting.

Of all tested membranes the Spectra/Por 3.5-5 kDa MWCO RC membrane from SpectrumEurope (Breda, NL) turned out to be the most consistent; however, for shorter experiments a better membrane has to be found.

3.4 Summary and Outlook

Two prototypes of OPC provided by Anton Paar GmbH (Graz, Austria) were tested during this Master's thesis. The second prototype successfully retained enough sample within the x-ray beam for detecting MLV scattering. Obtained d-values are in good agreement with the calibration curve (Fig. 3.12), highly encouraging further work on this system. Limiting issues which need to be over come are (i) equilibration time and (ii) sealing against vacuum during pressure relaxation experiments. To further improve the performance of the OPC some suggestions are made in this section. Their major purpose is to reduce equilibrium time and enhance durability. Described upgrades are relating to lipid MLVs measurements. Testing other colloids like silica nanobeads or clay minerals should be taken into consideration.

3.4.1 Upper Seal

For better sealing properties the shape of the upper housing seal should be redesigned using an elastomer with a thickness of 2 mm as shown in Fig. 3.13.

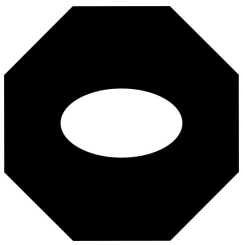

Figure 3.13: Due to the new shape, compared to the old design in Fig. 1.7, the seal stays in place and excess elastomer, created by tightening of the seal, can move to the corners. This prevents blocking the whole in the middle. A material thickness of 2 mm is recommend to increase leakage proof in pressure ramp experiments.

3.4.2 Pressure System

In order to ease setting the pressure, a digital control should be implemented. Precise pressure ramps can be performed and processes to flush the semipermeable membrane pores can be realized. Another improvement to the existing systems would be an extended water reservoir outside of the vacuum chamber which would allow monitoring water displacement during the ongoing experiment and can help detecting leakage of the lower compartment (water reservoir under the semipermeable membrane). In case of leakage water would be sucked from the outside reservoir to the inside of the vacuum chamber and this indicates a seal defect.

3.4.3 Membrane Test Station

The experiment duration depends mainly on the semipermeable membrane; however, the requirements change with every different sample. Therefore, a test bench which allows simultaneously testing of several membranes in the lab would be a great achievement. Also pretreatments like washing could be performed in such a station.

3.4.4 Cell Design

Upcoming redesign of the osmotic pressure cell should consider even more sample above the x-ray window and higher flow rate. Temperature control can be implemented into the cell housing. The support frit should be changed to a hemisphere or a similar shape to increase the semipermeable membrane's surface. Additionally, membrane covered walls and a flushing or mixing (ultrasonic) system should be considered. An idea for a new designs is using a supported semipermeable membrane balloon (connected to the pressure system with a hose) in a water reservoir. A SAXS measurement could be performed right through the balloon and its support (Fig. 3.14).

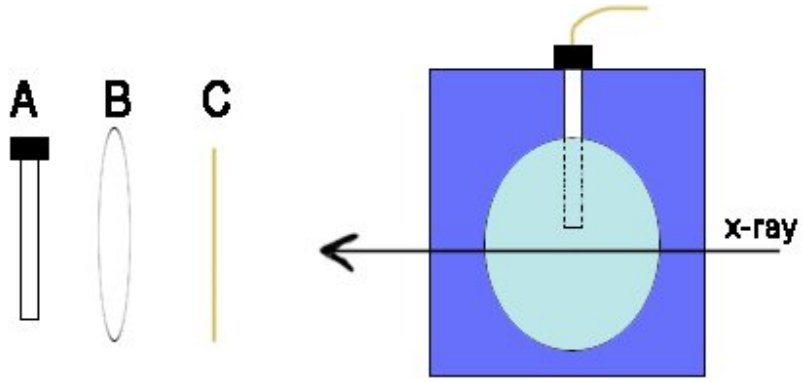

Figure 3.14: A possible alternative to set osmotic pressure is a semipermeable membrane balloon. The balloon (B) itself is deflated at the beginning. The sample is loaded into the pipe (A) and afterwards the pipe is inserted into the empty balloon and sealed. Using quick connectors the pipe is connected to the pressure hose (C). Next, the balloon is placed into a housing with a water pool (reservoir) and x-ray windows similar to the OPC. The water pool is connected to the reference pressure outside the vacuum chamber. A set pressure loads the sample from the pipe into the balloon and excess water can penetrate through the semipermeable membrane to reach osmotic equilibrium. For low pressures the balloon can be placed in the water pool without further support due to the mechanical strength of the membrane. However, for higher pressures a cage or net around the balloon is needed - or the OPC cell is used.

Bibliography

[1] G. Binnig, C. F. Quate, and and Ch. Gerber. "Atomic Force Microscope." In: *Phys. Rev. Lett.* (1986), pp. 930–933.

[2] J. Israelachvili et al. "Recent advances in the surface forces apparatus (SFA) technique." In: *Reports on Progress in Physics* 73.3 (2010). DOI: 10.1088/0034-4885/73/3/036601.

[3] Gerrit Sitters et al. "Acoustic force spectroscopy." In: *NATURE METHODS* 12.1 (2014), pp. 47–50. ISSN: 1548-7091. DOI: 10.1038/nmeth.3183.

[4] D. M. Le Neveu, R. P. Rand, and V. A. Parsegian. "Measurement of forces between lecithin bilayers." In: *Nature* 259 (1976), pp. 601–603.

[5] J. DeRouchey, V. A. Parsegian, and D. C. Rau. "Cation charge dependence of the forces driving DNA assembly." In: *Biophysical Journal* 99.8 (2010), pp. 2608–2615. ISSN: 0006-3495.

[6] Antoine Bouchoux et al. "How to squeeze a sponge: casein micelles under osmotic stress, a SAXS study." In: *Biophysical Journal* 99.11 (2010), pp. 3754–3762. ISSN: 0006-3495. DOI: 10.1016/j.bpj.2010.10.019.

[7] Benjamin Kollmitzer et al. "Bending Rigidities and Interdomain Forces in Membranes with Coexisting Lipid Domains." In: *Biophysical Journal* 108.12 (2015), pp. 2833–2842. ISSN: 0006-3495. DOI: 10.1016/j.bpj.2015.05.003.

[8] Eric Raspaud. "An alternative method to the osmotic stressing polymers: The osmomanometer." In: *European Biophysics Journal* 32.4 (2003), pp. 402–404. ISSN: 01757571. DOI: 10.1007/s00249-003-0304-0.

[9] B.L.L.E. Gauthé et al. "A high pressure cell for simultaneous osmotic pressure and x-ray diffraction measurements." In: *Rev Sci Instrum* 80 (2009), p. 35107.

[10] S. Tristram-Nagle, H. I. Petrache, and J. F. Nagle. "Structure and interactions of fully hydrated dioleoylphosphatidylcholine bilayers." In: *Biophysical Journal* 75.2 (1998), pp. 917–925. ISSN: 0006-3495.

[11] *Avanti Polar Lipids, Inc.* 2018. URL: https://avantilipids.com/product/850375/.

[12] R.A.L. Jones. *Soft Condensed Matter*. Oxford Master Series in Physics. OUP Oxford, 2002. ISBN: 9780198505891.

[13] Jacob N. Israelachvili. *Intermolecular and surface forces*. 3rd ed. Burlington, MA: Academic Press, 2011. URL: http%3A//www.worldcat.org/oclc/706803091.

[14] V. A. Parsegian. *Van der Waals Forces*. New York, NY: Cambride University Press, 2004.

[15] *Wikipedia Covalent bond*. 2018. URL: https://en.wikipedia.org/wiki/Covalent_bond.

[16] *Wikipedia Solvation*. 2018. URL: https://en.wikipedia.org/wiki/Solvation.

[17] Ole G. Mouritsen. *Life - as a matter of fat: The emerging science of lipidomics*. Berlin: Springer, 2005.

[18] Daniel Harries and Uri Raviv. "Soft matter physics of lipid membrane-based assemblies." In: *Liposomes, Lipid Bilayers and Model Membranes*. Ed. by Georg Pabst et al. Boca Raton, FL: CRC Press, 2014, pp. 3–30.

[19] M. Rappolt and G. Pabst. "Flexibility and Structure of Fluid Bilayer Interfaces." In: *Structure and Dynamics of Membranous Interfaces*. Ed. by K. Nag. Hoboken, NJ: Wiley, 2008, pp. 45–82.

[20] A. Guinier and G. Fournet. *Small-angle scattering of X-rays*. Structure of matter series. Wiley, 1955.

[21] O. Glatter and O. Kratky, eds. *Small Angle X-ray Scattering*. London, UK: Academic Press, 1982. ISBN: 0-12-286280-5.

[22] H. I. Petrache, D. Harries, and V. A. Parsegian. "Measurement of lipid forces by X-ray diffraction and osmotic stress." In: *Methods Mol Biol* 400 (2007), pp. 405–419. ISSN: 1064-3745.

[23] D. G. Hunter and B. J. Frisken. "Effect of Extrusion Pressure and Lipid Properties on the Size and Polydispersity of Lipid Vesicles." In: *Biophysical Journal* 74.6 (1998), pp. 2996–3002. ISSN: 0006-3495. DOI: 10.1016/S0006-3495(98)78006-3.

[24] *Spectrum Labs*. 2018. URL: http://spectrumlabs.com/dialysis/PoreSize.html.

[25] *Altmann Analytik GmbH*. 2018. URL: https://www.analytics-shop.com/de/.

[26] *Sigma-Aldrich Co.* 2017. URL: www.sigmaaldrich.com.

[27] Christopher B. Stanley and Helmut H. Strey. "Measuring Osmotic Pressure of Poly(ethylene glycol) Solutions by Sedimentation Equilibrium Ultracentrifugation." In: *Macromolecules* 36.18 (2003), pp. 6888–6893. DOI: 10.1021/ma034079e.

[28] Georg Pabst et al. "Entropy-Driven Softening of Fluid Lipid Bilayers by Alamethicin." In: *Langmuir* 23.23 (2007), 11705\textendash11711. DOI: 10.1021/la701586c.

Appendix

Matlab Code

Loading SAXS data and finding peak position:

```
function[q,i,e,pks,locs] = load_pdh(filename,qmax,
    MinPeakHeight)
z=qmax; %Anzahl der Zeilen
fid=fopen(filename,'r');
if fid<0
    error(['Could not load: ' filename])
end
%pks=nan(3,1);
%locs=nan(3,1);
data=textscan(fid,'%f %f %f',z,'HeaderLines',5,'
    Delimiter',{'\t','\t','\n'});

q=data{1};
i=data{2};
e=data{3};
[pks,locs] = findpeaks(i(:,1),'MinPeakHeight',
    MinPeakHeight);
if size(pks) == [3,1]
else
    pks=zeros(3,1);
    locs=zeros(3,1);
end
fclose(fid);
```

Gaussian fit for d-spacing:

```
clear all; close all; format long;
function [xdraw,dist2,q,i]=d_spacing();
filename1=('C:\SAXS\FOLDER\example\SDD_308mm.001\
    SDD_308mm.001_averaged_corrected.pdh');
prompt = 'What is the total amount of files?';
result = input(prompt);
MinPeakHeight = 0.5; %Min.  Height of peaks to find
    first and second order
```

```
%Only data with peak information; without noise: e.g. q=3
[qstart,istart,estart]= read_SAXdata_start(filename1);
qmax=length(qstart(qstart<3));

% Getting Data and peak locations
for j=1:result
filename=([ 'C:\SAXS\FOLDER\example\SDD_308mm.' num2str(j,'%03d') '\XY__SDD_308mm.' num2str(j,'%03d') '_averaged_corrected.pdh']);
if j==xxx %%%%%%%% For Problem reading peaks file at file xxx
    MinPeakHeight = 0.4; % change minimum peak height
end
[q(:,j),i(:,j),e(:,j),pks(:,j),locs(:,j)] = read_SAXdata(filename,qmax,MinPeakHeight);
end
%kicking out data bad measurements
logic1=pks~=0; logic=logic1(1,:);
[qnew,sizebefore]=size(q);
q=q(:,logic); i=i(:,logic); e=e(:,logic);
pks=pks(:,logic); locs=locs(:,logic);
[qnew,sizeafter]=size(q);
kickedout=sizebefore-sizeafter

%Gaussian fct. a[..] Parameter, x = data;
F = @(a,x) a(1).*exp(-((x-a(2)).^2)./ (2*a(3).^2))+a(4);
[pmax,qnew]=size(pks);
pwidth=[0.5,0.1,0.1];        %fitting width
a21=[0,1,2];  %mean peak
aopt=nan;

for peak=2:pmax  %fitting for n=2 order
for n=1:result-kickedout
qpeak=q(locs(peak,n),n); %max. value of peaks
q1=q(:,n);
```

```
38 i1=i(:,n);
39 qg=q1(q1>qpeak-pwidth(peak) & q1<qpeak+pwidth(peak));
                %q for Gaussian
40 ig=i1(q1>qpeak-pwidth(peak) & q1<qpeak+pwidth(peak));
                %i for Gaussian
41
42 if(n==1)
43 a1(n)=(max(ig)-min(ig));       %amplitude height
44 a2=a21(peak);                          %peak shift
45 a3= pwidth(peak);          %point of inflection distance
46 a4=min(ig);                    %offset
47
48 ag(:,n)=[a1(n),a2,a3,a4];
49 [ag(:,n),resnorm,~,exitflag,output] = lsqcurvefit(F,ag
      (:,n),qg,ig);
50 else
51 %Solving fct.
52 [ag(:,n),resnorm,~,exitflag,output] = lsqcurvefit(F,ag
      (:,n-1),qg,ig);
53 end
54 qplot=linspace(qg(1),qg(end),1000);
55 [qnew,posq]=max(F(ag(:,n),qplot));
56 qfinal(n,peak)=qplot(posq);
57
58 %% Plotting data points with Gaussian fit for visiual
      control
59  figure(n+100*peak)
60  semilogy(q(:,n),i(:,n),'.')
61  hold on
62  semilogy(qplot,F(ag(:,n),qplot),'-r')
63 pause(0.05)
64  hold  off
65 end
66 end
67 dist1=2*pi./qfinal(:,2)*10;
68 dist2=4*pi./qfinal(:,3)*10;
69 xdraw=(1:numel(dist2));
```